



Performance Characterization of Lithium-Ion Battery and Ageing Under Constant Stress Conditions at Low Temperature

Ossama Rafik, Armande Capitaine, Olivier Briat and
Jean-Michel Vinassa

EasyChair preprints are intended for rapid
dissemination of research results and are
integrated with the rest of EasyChair.

July 22, 2024

Performance characterization of lithium-ion battery and ageing under constant stress conditions at low temperature

O. Rafik^{a,*}, A. Capitaine^a, O. Briat^a, J.-M. Vinassa^a

^a Univ. Bordeaux, CNRS, Bordeaux INP, IMS, UMR 5218, F-33400 Talence, France

Abstract

This paper presents a comparison on cycling strategies for lithium-ion batteries. Furthermore, an evaluation of two cycling strategies is conducted on an experimental study on LG 21700 lithium-ion battery. The investigation focused on examining the capacity degradation on batteries subjected to two cycling protocols, conducted at an ambient temperature of 0°C and stress factors depend on actual capacity instead of nominal capacity. The capacity losses were estimated after cycling and were found to be 27% for protocol 1, and 20% for protocol 2. This paper also presents the impact of discharging current and the depth of discharge on capacity utilization to support the development of optimized cycling protocols for practical applications

1. Introduction

The lifespan of the battery depends on the conditions of use; hence an accelerated aging test is possible instead of a real use profile because it would take too much time. Accelerated aging serves as a cost-effective and efficient approach, providing cycling data in a short timeframe (days to months). This capability allows the prediction of the lifespan of Lithium-ion Batteries (LIBs) under diverse operational stresses. During accelerated aging testing, it is crucial to analyse the aging mechanisms of the battery, our objective is to focus on a specific degradation mechanism, as lithium plating, and to develop a dedicated accelerated aging tests to address it.

Lithium plating refers to the reduction of dissolved Li^+ ions in the electrolyte to form metallic lithium on the surface of the anode's active material. This reaction occurs instead of the usual intercalation of lithium into the lattice structure of the active material [1].

For ease of use, the accelerated stress factors typically employed include ambient temperature (T), current rates (C-rate), state of charge (SOC), and depth of discharge (DOD). The C-rate stands as a crucial parameter in assessing battery usage cycles. It quantifies the rate at which a battery is discharged relative to its nominal capacity (a 1C rate indicating that the discharge current will discharge the entire battery in 1 hour). Eddahech et al [2] proposed an equivalent-circuit model for the impedance of the battery, in order to identify the main factors of ageing, the authors considered the C-rate, SOC and the cell

temperature as the main factors of ageing in the case of power cycling. Vries et al [3] considered depths of discharge, with up to four series of charge-discharge experiments. The authors found that the cycle life increase as the DOD is reduced or as the same amount of charge is extracted from a lower SOC.

In lithium-ion batteries, the conversion between electrical energy and chemical energy is achieved through repeated lithium-ion intercalation and deintercalation. Side chemical reactions can cause irreversible losses of electrolyte, active electrode materials, and lithium inventory; therefore, the capacity decreases over cycles [4].

Studies have shown that the build-up of solid electrolyte interphase (SEI) and lithium-plating passive film layers on the anode electrode occur due to the depletion of cyclable lithium ions [5,6]. The formation of a thick, uneven passive film on the material's surface decreases electrode porosity and blocks the flow of lithium ions, leading to increased resistance and reduced capacity over time [7]. Therefore, any cycling procedure for lithium-ion batteries must consider these underlying limitations to ensure safe operation and an extended cycle life. Hence, subjecting the battery to cycling with stress factors that are determined by the nominal capacity rather than the actual capacity, which decrease over time, results in an increase in stress that intensifies with the aging process.

Despite the variety of publications detailing cycling lithium-ion batteries under diverse conditions, there is limited information available on how degradation processes evolve when discharge rates are lowered. In other words, most existing

degradation models are only validated after cycling the battery under nominal discharge currents.

Nevertheless, up to now, there was very few interests, if any, in examining how the performance parameters of the battery are influenced by the operational conditions associated with the real state of the battery, rather than its nominal state. Therefore, in this study, we present a comparison of the battery performance and its reliance on the operational conditions at two distinct levels of degradation. This comparison follows extensive aging tests, where the discharge current rate and depth of discharge depend on the actual capacity of the battery, not the nominal.

2. Experimental

2.1. Lithium-ion cell characteristics

The tested cells are lithium-ion NMC811-4.85Ah elements in the standardized 21700 cylindric format. Their main characteristics are presented in the table 1.

Table 1
Characteristics of the tested cells

Manufacturer	LG Chem
Model	INR21700 M50
Nominal capacity C_N	4.85 Ah
Maximum voltage V_{max}	4.2 V
Minimum voltage V_{min}	2.5 V
Standard charging current	1.455 A
Anode material	Graphite SiO_x
Cathode material	$Li(Ni_8Mn_1Co_1)O_2$

2.2. Test procedure

The experimental tests were conducted using a Biologic BCS-815 electrochemical workstation equipped with 8 channels, each capable of handling charge-discharge currents up to 15A. Furthermore, this equipment allows to perform Electrochemical Impedance Spectroscopy (EIS) measurements. Then, a climatic chamber is used to impose the ambient temperature. Before the cycling procedure and every 90 cycles, a detailed characterization test (check-up) is made on each cell at an ambient temperature of 25°C. These check-ups consist in a constant current – constant voltage (CC–CV_N) in ord charge followed by a constant current discharge of 0.97A (C-rate of 0.2C_N) in order to measure the remaining capacity of the cell. Then, the cells are charged up to 50% of the previously determined capacity. Finally, after a rest period of 1h, EIS measurement on the frequency range [2kHz-100mHz]_{DC} and charge-discharge pulses

test are made to determine the impedance and the equivalent series resistance (ESR_{DC}, 10s after current pulse interrupt) at 50% of SOC.

2.3. Ageing protocols

The investigated ageing tests are based on two cycling protocols and an ambient temperature of 0°C. For the protocol P1, the battery is discharged every cycle with a constant current of 2.425 A (0.5C_N) until 50% of the actual capacity C_A is reached. The actual capacity C_A is determined every 30 cycles with a constant current discharge of 0.2C_N down to a cut-off voltage of 2.5V and at the ageing temperature (0°C). For protocol P2, the battery is discharged every cycle until 0.5C_A is reached, but C_A is reached, but unlike P1, the current is related to the actual capacity C_A measured in the same conditions as for the protocol P1.

3. Results and discussion

3.1. Evolution of the performance indicators

The energy and power performance of a battery are linked to the capacity (Q) and to the internal resistance (R), respectively. To study the evolution of these two quantities with ageing, Q and R are determined periodically by characterization tests (check-up) made at 25°C ambient temperature. The average of the capacity and resistance for two cells, cycled under the same conditions, are shown in and respectively. The evolution of these performance indicators is represented in Figure 1 and 2, for the two cycling protocols, as a function of the discharge capacity throughput, which corresponds to the cumulated charge passing through the cell during the discharge.

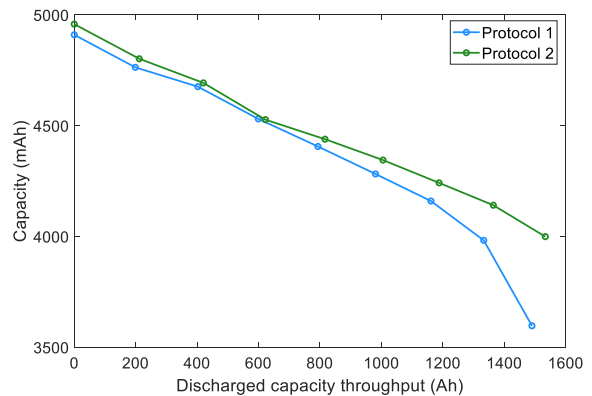


Fig. 1. Comparison of the capacity loss versus discharged Ah throughput, for the two cycling protocols.

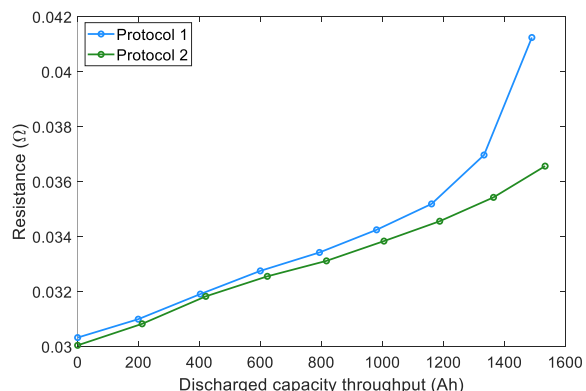


Fig. 2. Comparison of ESR_{DC} increase versus discharged Ah throughput, for the two cycling protocols.

These results highlight a two-step performance degradation both on the capacity loss and on the resistance growth. Up to a discharged capacity throughput of 800Ah, the degradation rate of the two indicators remains almost constant and equal for the two protocols. Then, this degradation rate increases significantly for protocol 1, leading to a divergence on the evolution of both the capacity and the resistance with ageing.

Cells cycled under protocol (P1) degraded rapidly, reaching 73% of their initial capacity with an average throughput of 1490 Ah and a resistance increase of 1.36. In contrast, cells cycled under protocol (P2) exhibited a slower degradation rate at the same state of charge (SOC) of 50%, reaching 80% of their initial capacity with a throughput of 1540 Ah and a resistance increase of 1.21.

3.2. Electrochemical impedance spectroscopy

Electrochemical Impedance Spectroscopy (EIS) measurements are conducted at the start and end of cycling tests to monitor changes in internal resistances. These measurements involve potentiostatic measurements taken across a frequency range of 2 kHz to 100 mHz, while maintaining a State of Charge (SOC) of 50%. The excitation voltage used is $V_{ac} = 10$ mV.

Figure 3 show impedance spectra for two different cycling protocols in initial and final states. Protocol 2 cells have the lowest increase in internal resistances, while Protocol 1 cells have the highest. The spectra include two semicircles at high and mid frequencies, and a low-frequency tail. The high-frequency resistance is linked to the current collector and remains stable with aging.

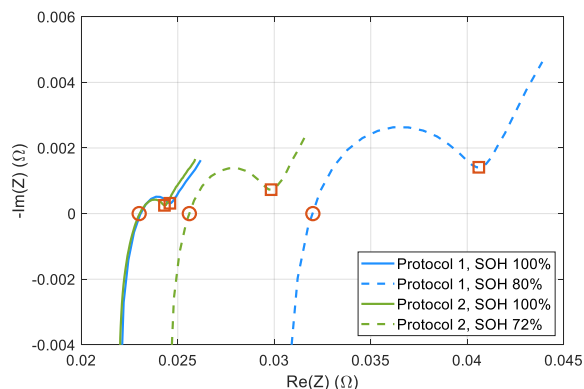


Fig. 3. Impedance spectra of new and cycled cells under P1 and P2 at SOC 50%, ranging from 2kHz to 100 mHz.

The upper segment of the spectrum includes a distorted semicircle and a sloping line. The semicircle represents effects from passivation layers, charge transfer resistances, and double layer capacities, while the sloping line indicates limitations in mass transport due to diffusion processes. X markers are used to mark the cell impedance at 1 Hz, with the real part denoted as R_{ct} showing changes in internal resistances and used in cycle life studies as an indicator of effects from charge transfer and diffusion processes.

The size of mid-frequency semicircles in porous electrodes can vary, pointing to differences in interfacial properties. Factors such as local resistances, surface alterations of active materials, and decreased porosity can impact charge transfer resistances and double layers.

Circular markers represent ohmic behavior in a circuit, where the impedance is purely real and equal to zero. This real part is referred to as R_0 and is influenced by factors like electrolyte conductivity and metal conductor resistances. R_0 is calculated by interpolating between frequency points above and below the x-axis.

3.3. Resistance growth

As cells age, their internal resistance often increases due to the build-up of side reaction products on the electrode particles. Under constant current conditions, the additional overpotential from increased internal resistance will cause the cell to reach the cut-off voltage more quickly as shown in Figure 5, decreasing the capacity, energy, and power per cycle. The differences in the delivered energy can be explained due to changes of temperature as shown in Figure 4.

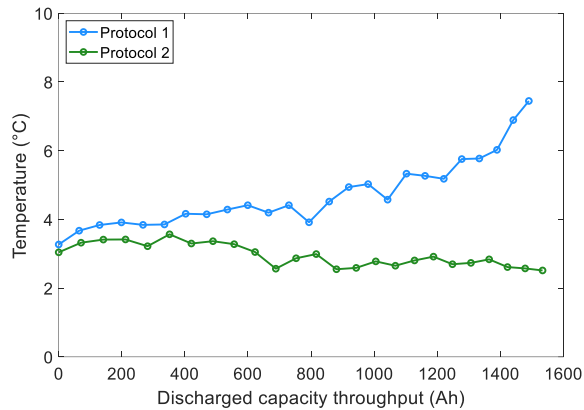


Fig. 4. Evolution of the cell temperature vs discharged capacity

The magnitude of this overpotential growth rate is a product of both the resistance growth rate and the applied current. Decreasing the discharge current and the DOD leads to a constant temperature for protocol 2 instead of protocol 1.

In lithium-ion batteries, the voltage-capacity curves exhibit relatively flat slopes at higher voltages or states of charge (small dV/dQ), contrasting with steeper slopes at lower voltages or states of charge (large dV/dQ).

During cycling at low rates, the charge capacity is highly sensitive to increases in resistance, while the discharge capacity is less affected until reaching a certain point on the voltage-capacity curve. At this point, the discharge capacity becomes more sensitive to changes in overpotential, leading to a decrease in capacity, energy, and power.

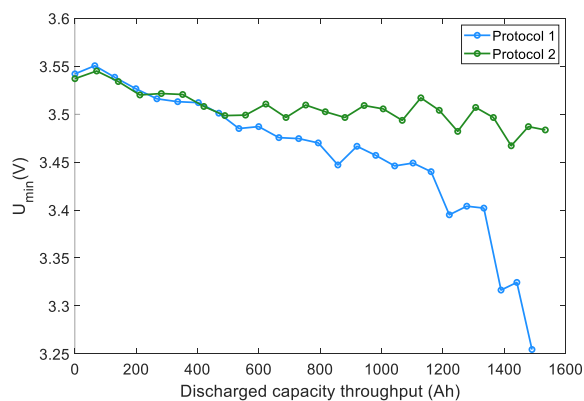


Fig. 5. Evolution of the lower cut-off voltage vs discharged capacity.

4. Conclusion

A study was conducted on LGM50 21700 lithium-ion batteries using different cycling protocols to determine their impact on cycle life. The results showed that Protocol P2, which maintained constant DOD and C-rate conditions, led to the longest lifespan

with less capacity decay and delayed impedance increase compared to Protocol P1.

The relationship between resistance growth and measured capacity during battery aging is affected by discharge rate and lower cut-off voltage. Lowering discharge rates and cut-off voltage can delay aging by reducing overpotential. Energy and power are more affected by discharge rate than capacity, so cycling at lower rates or to lower cut-off voltage can delay aging

References

- [1] V. Zinth, C. von Lüders, M. Hofmann, J. Hattendorff, I. Buchberger, S. Erhard, J.Rebello-Kornmeier, A. Jossen, R. Gilles, Lithium plating in lithium-ion batteries at sub-ambient temperatures investigated by in situ neutron diffraction, *J.Power Sources* 271 (2014)
- [2] A. Eddahech, O. Briat, H. Henry, J.-Y. Delétage, E. Woïrgard, J.-M. Vinassa, Ageing monitoring of lithium-ion cell during power cycling tests, *Microelectronics Reliability* 51, (2011) 1968-1971.
- [3] H.Vries, T.Nguyen, B.Veld, Increasing the cycle life of lithium ion cells by partial state of charge cycling, *Microelectronics Reliability* 55 (2015) 2247-2253
- [4] X.Hu,L.Xu,X.Lin,M.Pecht, Battery Lifetime Prognostics, *Joule* 4, (2020) 310–346.
- [5] W.Huang, P. Attia, H.Wang, S.Renfrew, N.Jin, S.Das, Z.Zhang, D.Boyle, Y.Li, M.Bazant, B.McCloskey, W.Chueh, Y.Cui, Evolution of the Solid–Electrolyte Interphase on Carbonaceous Anodes Visualized by Atomic-Resolution Cryogenic Electron Microscopy, *Nano Letters* 19 (2019) 5140-5148
- [6] M.Pinson, M.Bazant, Theory of SEI Formation in Rechargeable Batteries: Capacity Fade, Accelerated Aging and Lifetime Prediction, *J. Electrochem. Soc* (2013) . 160 A243
- [7] X.Yang, Y.Leng, G.Zhang, S.Ge, C.Wang, Modeling of lithium plating induced aging of lithium-ion batteries: Transition from linear to nonlinear aging, *J.Power Sources* 360 (2017) 28-40,